Table of Contents

Materials

Chemicals. Sodium hyaluronate (mW ≈ 30 kDa) was purchased from Bloomage Biotech. (Beijing, China). Cerium (III) nitrate hexahydrate, hydrogen peroxide solution (30 wt.% H_2O_2), amiloride hydrochloride, genistein, chlorpromazine, and paraformaldehyde solution (4 wt.% PFA) were purchased from Titan Biotech. (Shanghai, China). 1-(3-Dimethylaminopropyl)-3-ethylcarbodiimide hydrochloride (EDC), 1-hydroxybenzotriazole (HOBT), mercaptolethylamine hydrochloride, 2',7'-dichlorodihydrofluorescein diacetate (DCFH-DA), and Annexin V-fluorescein isothiocyanate (FITC) apoptosis detection kit were purchased from Aladdin Biochem Tech. (Shanghai, China). Benzalkonium chloride (BAK) and scopolamine (SCOP) were purchased from Sigma-Aldrich (St. Louis, USA). Rosmarinic acid was purchased from Meryer Biotech. (Shanghai, China). ABTS free radical scavenging capacity assay kit was purchased from Solarbio Biotech. (Beijing, China). 10 mM phosphate buffered saline (PBS), Dulbecco's modified eagle medium (DMEM), and 1% penicillin/streptomycin were purchased from Thermo Fisher Scientific (MA, USA). 10% Fetal bovine serum (FBS)-Premium were purchased from NEWZERUM (Christchurch, New Zealand). Triton-X 100 solution, Actin-Tracker Red-594, Bradford protein assay kit, and live/dead viability/cytotoxicity assay kit were purchased from Beyotime Biotech. (Shanghai, China). Cell counting kit-8 (CCK-8) was purchased from Life-iLab (Shanghai, China). Mucin, lipopolysaccharide (LPS), and Total antioxidant capacity assay kit with ferric reducing ability of plasma (FRAP) method were purchased from Yuanye Bio-Tech. (Shanghai, China). 4',6-diamidino-2-phenylindole (DAPI) was purchased from Yeasen Biotech. (Shanghai, China). Enzyme-linked immunosorbent assay (ELISA) kits of Transforming Growth Factor-β (TGF-β), Tumor Necrosis Factor-α (TNF-α), and Interleukin-6 (IL-6) were purchased from Solarbio Biotech. (Beijing, China).

The primary antibodies used in study were listed as follows: γ-Histone 2A.X (γ-H2A.X) antibody (Ser 139) (Santa Cruz, 1:1000, USA), inducible Nitric Oxide Synthase (iNOS) polyclonal antibody (Proteintech, 1:200), Arginase-1 (Arg-1) polyclonal antibody (Proteintech, 1:200), phycoerythrin (PE)-conjugated anti-mouse Cluster of Differentiation 86 (CD86) antibody (Thermo Fisher Scientific, 1:200, USA), allophycocyanin (APC)-conjugated anti-mouse CD206 antibody (BioLegend, 1:200, USA), Interleukin-6 (IL-6) monoclonal antibody (Proteintech, 1:200, USA), and Matrix Metallopeptidase-9 (MMP-9) polyclonal antibody (Proteintech, 1:200, USA). The secondary antibodies used in this study were listed as follows: HRP-conjugated Goat anti-Rabbit IgG (Proteintech, 1:5000), CoraLite 488-conjugated Goat anti-Rabbit IgG (Proteintech, 1:2000), and CoraLite 594-conjugated Goat anti-Rabbit IgG (Proteintech, 1:2000).

Cells and animals. Mouse macrophage cells (RAW264.7) and Human Corneal Epithelial Cells (HCECs) were purchased from American Type Culture Collection (ATCC). The animal experiments conducted in this study were carried out according to the guidelines set forth by the Association for Research in Vision and Ophthalmology Statement for the Use of Animals in Ophthalmic and Vision Research, as well as the Animal Care and Use Committee at Zhejiang University. Approval for these experiments was obtained from the Animal Ethics Committee at the Second Affiliated Hospital, School of Medicine, Zhejiang University (Approval number: 2024-284). All C57BL/6 mice (6-8 weeks, 20 ± 2 g) were provided by SLAC Laboratory Animal Co., Ltd (Shanghai, China). The mice were maintained in a controlled environment featuring a stable temperature and a standardized light/dark cycle, with unrestricted access to food and water.

Supplementary Methods

Characterizations. Zetasizer Nano ZS90 (Malvern Instruments, Worcestershire, UK) was utilized to measure the size distribution and surface ζ-potential of RHC NPs and *s*-RHC NPs. *In-situ* FTIR analysis of *p*-RosA was detected by an *in-situ* mid-infrared-based system React1R 15 (Mettler Toledo). The morphology and chemical compositions of NPs were observed by the Talos F200X field emission transmission electron microscope (TEM) (Thermo Fisher Scientific) at an accelerated voltage of 200 kV. Ultraviolet-visible spectra (UV-*vis*) were collected by the UV-2700 UV-vis spectrophotometer (Shimadzu). X-ray Photoelectron Spectroscopy (XPS) experiments were carried out using a Thermo ESCALAB 250XI spectrometer. Various kits (ABTS/MB/FRAP) were employed according to the instructions to evaluate the oxidation resistance of NPs.

Cell culture. RAW264.7 cells were cultured in Dulbecco's modified Eagle medium with 10% (v/v) fetal bovine serum and 1% penicillin/streptomycin. HCECs were cultured in Dulbecco's Modified Eagle Medium/Nutrient Mixture F-12 (DMEM/F12) medium with 10% (v/v) FBS and 1% penicillin/streptomycin. Both two types of cells were cultured at 37 °C in a humidified atmosphere containing 5% CO_2 and under recommended conditions.

Safety evaluation. Twenty mice were divided into four groups randomly and received topical instillation in the right eye of 5 μL of 0.9% saline (w/v), RosA, Ce^{3+}, RHC, and *s*-RHC (RosA: 200 μg/mL, Ce^{3+}: 60.8 μg/mL at a final concentration) twice per day for 14 consecutive days and their body weights were measured at a fixed time during the treatment period. On the last day of treatment, the mice's right eyes were monitored using a digital slit lamp. The OCT images were captured by immobilizing the anaesthetized mice onto the OCT device (Micron IV, Phoenix Research) and acquiring images during the scanning of the corneas' central region using the probe. Then, these mice were sacrificed by overdose anesthesia, and the right eyeballs of each mouse were carefully removed and processed into H&E sections.

Supplementary Figures

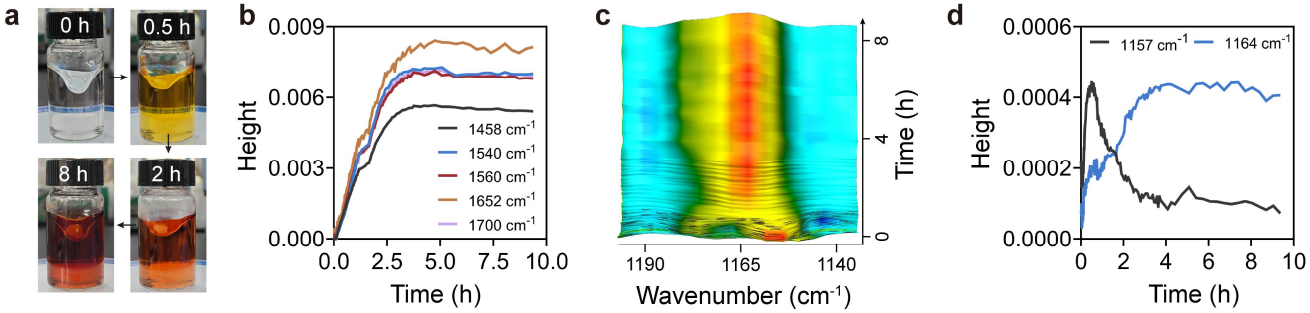

Supplementary Fig. 1. (a) Color change during the formation of *p*-RosA in solutions. (b) *In-situ* detection of peak changes in FTIR (1458, 1540, 1560, 1652, and 1700 cm^{-1}) which weighted by relevant heights. (c) *In-situ* FTIR spectra (1140 cm^{-1} ~ 1190 cm^{-1}) detecting the polymerization of RosA, and (d) the evaluation weighted by relevant heights (1157 and 1164 cm^{-1}).

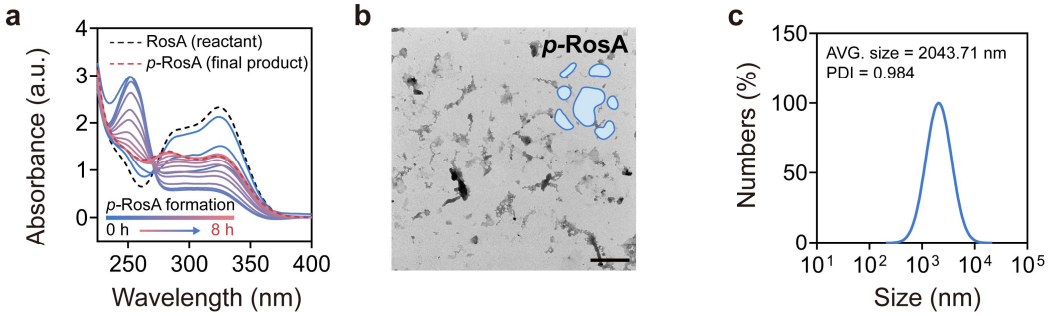

Supplementary Fig. 2. (**a**) Changes of UV-*vis* spectra during the formation of *p*-RosA in solutions. (**b**) The representative transmission electron microscopy (TEM) image and cartoon (inset) of *p*-RosA. Scale bar = 1 μm. (**c**) Hydrodynamic size distribution and PDI value of *p*-RosA solution.

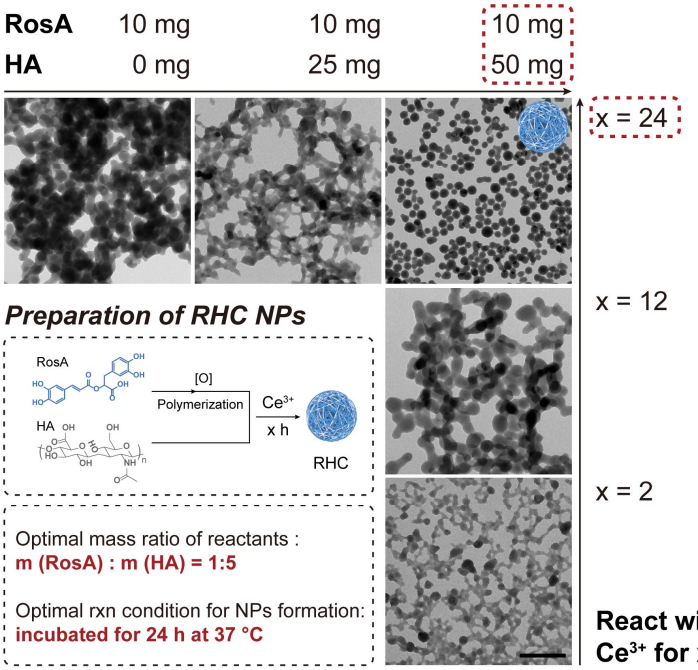

Supplementary Fig. 3. Representative TEM images and cartoon (inset) of RHC NPs synthesized under different conditions and the corresponding annotations. Scale bar = 500 nm.

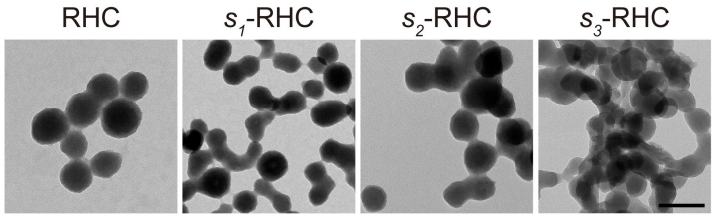

Supplementary Fig. 4. Representative TEM images of RHC NPs and three thiolated-RHC NPs. Scale bar = 300 nm.

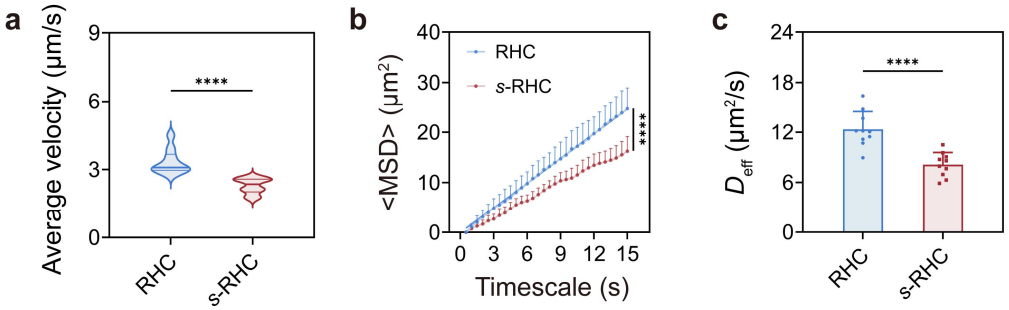

Supplementary Fig. 5. (**a**) Average velocity of RHC NPs and *s*-RHC NPs incubated with mucin solutions within 15 s. (**b**) Mean square displacement (MSD) values as a function of time scale for two kinds of NPs in mucin solutions. (**c**) Corresponding effective diffusion coefficient (D_{eff}) for two kinds of NPs in mucin solutions.

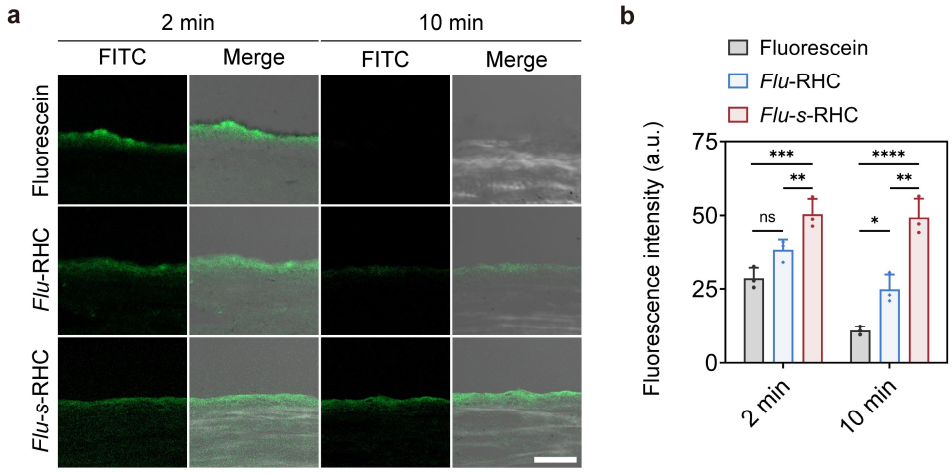

Supplementary Fig. 6. (**a**) Ocular surface frozen sections of mice, and (**b**) the quantitative assessment of average fluorescein intensity from ocular surface frozen sections of mice, which were administered free fluorescein, *Flu*-RHC NPs, and *Flu-s*-RHC NPs under conscious conditions for either 2 or 10 min (n=3), scale bar = 50 μm.

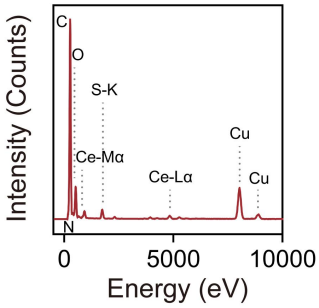

Supplementary Fig. 7. Energy dispersive spectrum (EDS) of *s*-RHC NPs.

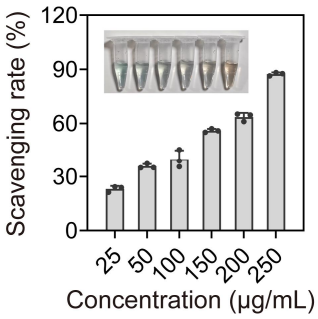

Supplementary Fig. 8. ABTS•+ scavenging ability of *s*-RHC NPs at different concentrations and the digital picture (inset) shown the color changes (n = 3).

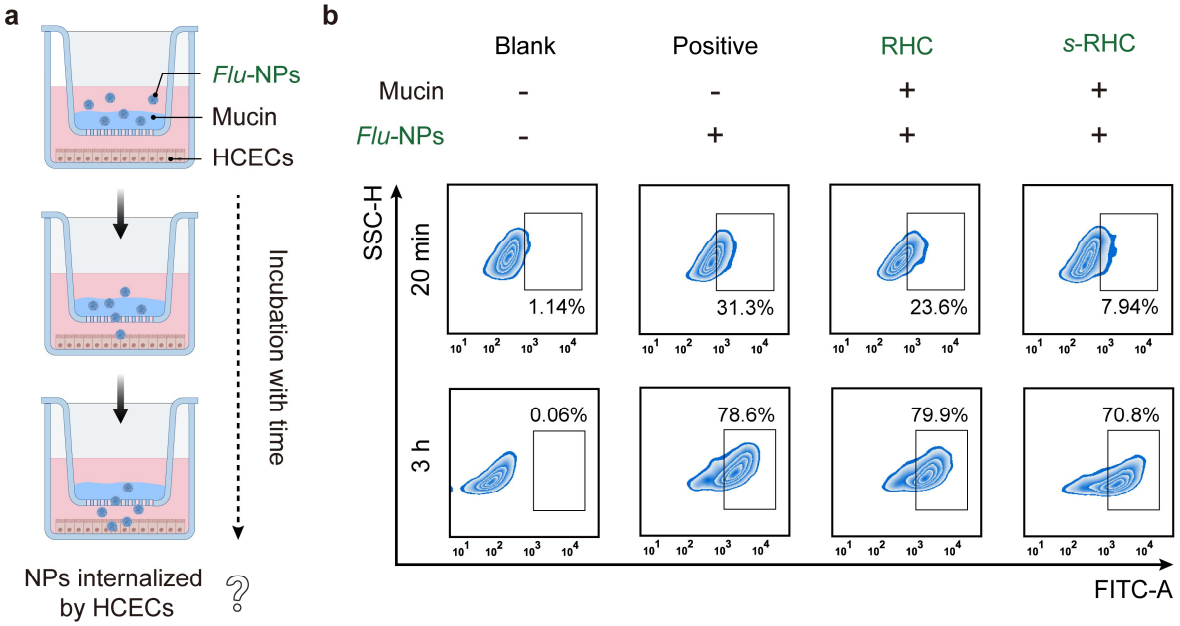

Supplementary Fig. 9.(**a**) Schematic diagram of HCECs monolayer transwell experiments mimicking the interactions between fluorescein-labelled NPs and ocular surface. (**b**) Group assignments and flow cytometry results of internalized formulations by HCECs cultured in the transwell at different time points (n = 3).

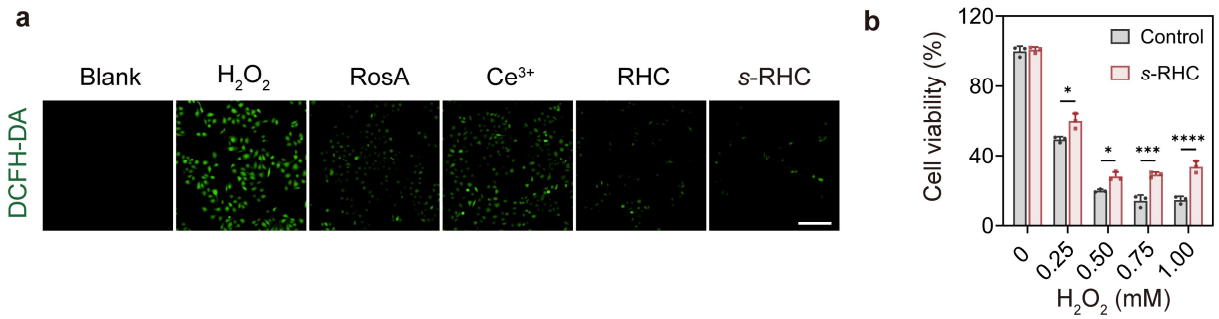

144

145 **Supplementary Fig. 10**. (**a**) Representative DCFH-DA fluorescence staining of HCECs after different treatments.

146 Scale bar = 100 μm. (**b**) Cell viability of different concentrations of H_2O_2-treated HCECs protected by *s*-RHC NPs (n

147 = 3).

148

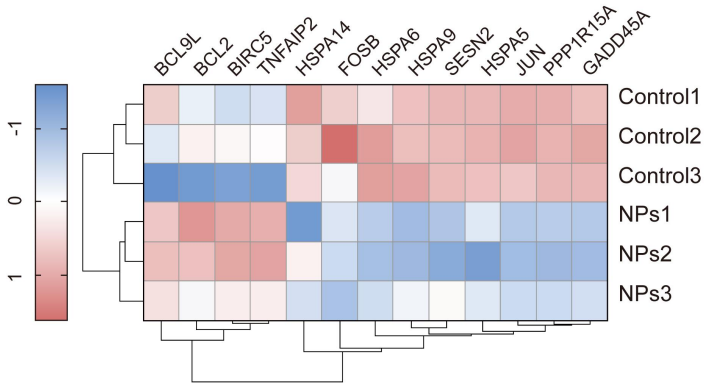

149

150 **Supplementary Fig. 11**. Representative normalized heatmap of hierarchical clustering showing the differential content

151 profiles of genes identified in different samples.

152

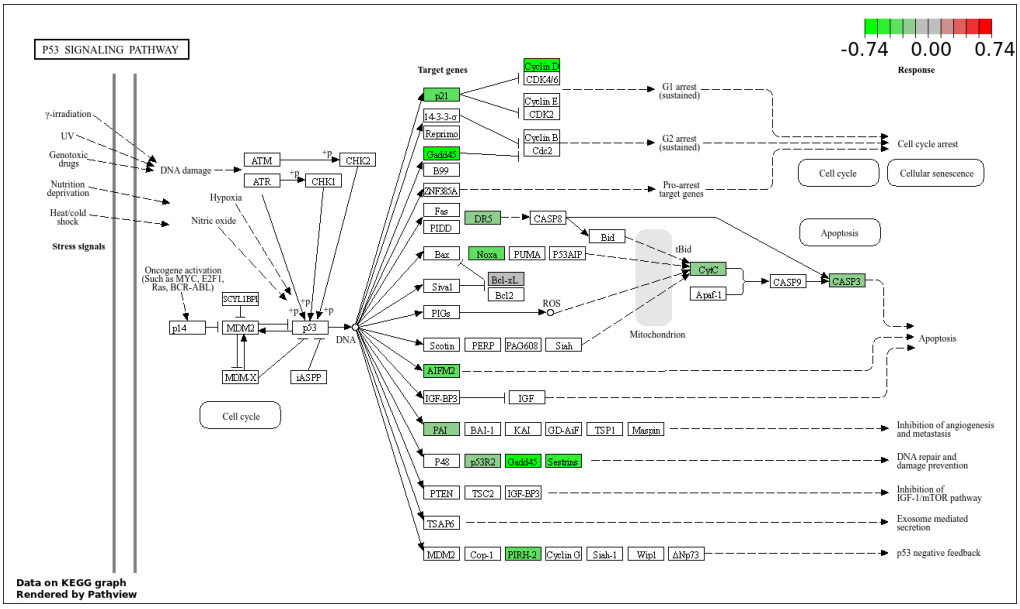

Supplementary Fig. 12. The specific change of gene expressions on P53 signaling pathway analyzed by KEGG enrichment. Darker red/green colors indicate higher levels of up-regulation/down-regulation, respectively.

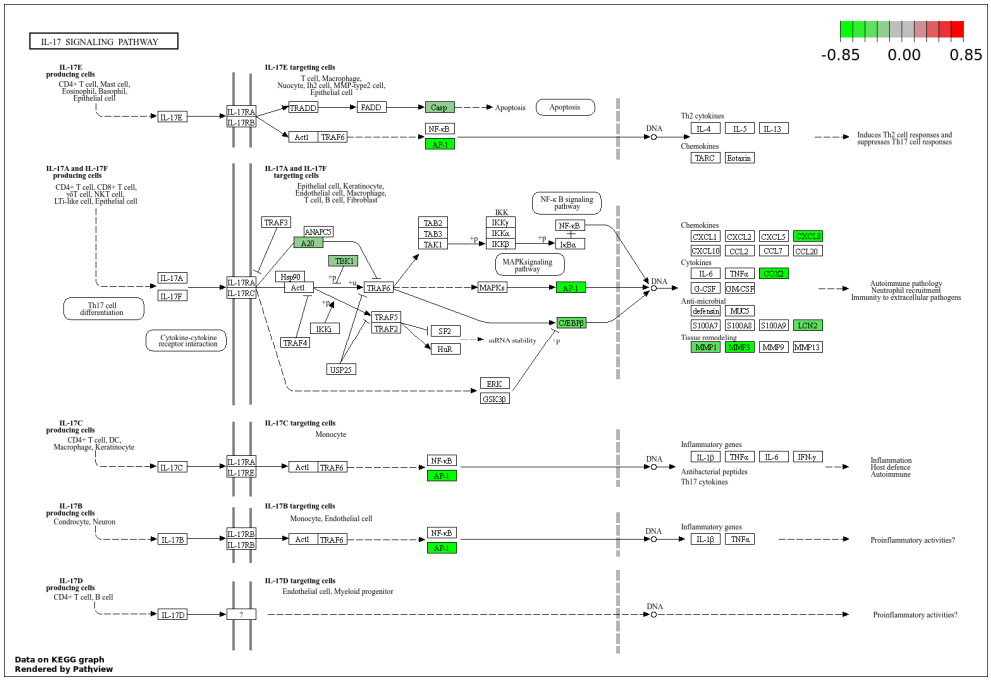

Supplementary Fig. 13. The specific change of gene expressions on IL-17 signaling pathway analyzed by KEGG enrichment. Darker red/green colors indicate higher levels of up-regulation/down-regulation, respectively.

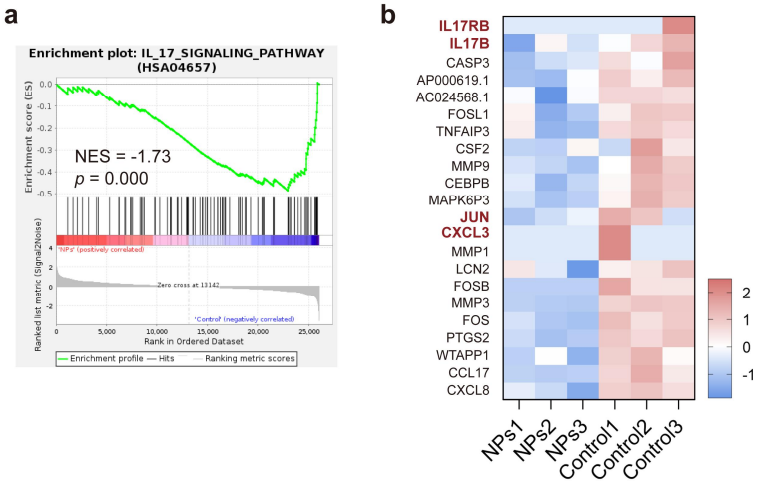

161

162 **Supplementary Fig. 14**. Results of (**a**) GSEA based on KEGG enrichment of significantly expressed signaling

163 pathways, and (**b**) normalized heatmap showing the differential content profiles of genes identified in IL-17 signaling

164 pathway.

165

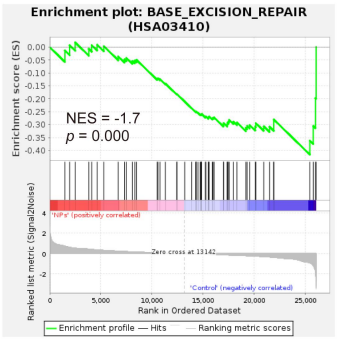

166

167 **Supplementary Fig. 15**. Results of GSEA based on KEGG enrichment of significantly expressed signaling pathways

168 (Base excision repair).

169

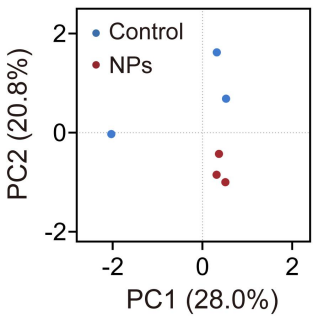

170

Supplementary Fig. 16. Principal component analysis (PCA) analysis presenting differentially expressed proteins expressed by H_2O_2-treated HCECs with or without *s*-RHC treatments (termed as "NPs" and" Control", respectively).

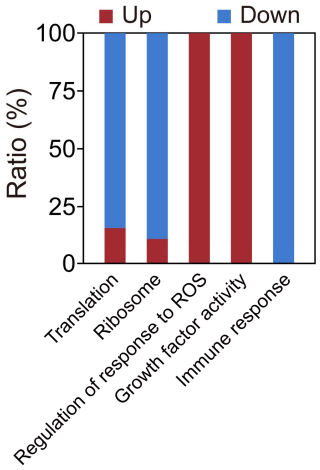

Supplementary Fig. 17. Bar graph illustrating the changes of differential proteins analyzed by Gene Ontology (GO).

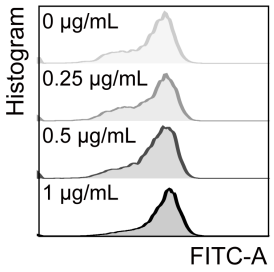

Supplementary Fig. 18. Results of intracellular ROS levels in RAW264.7 cells treated with varying LPS concentrations by flow cytometry.

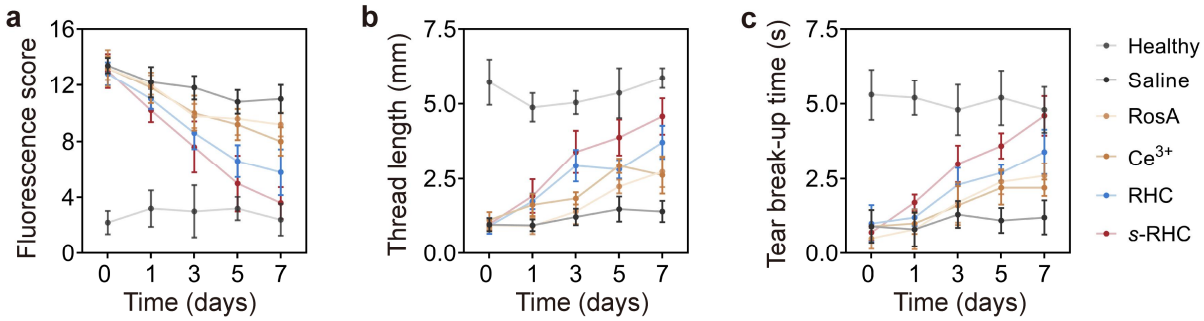

Supplementary Fig. 19. Records of (**a**) fluorescein staining score, (**b**) Schirmer measurement, and (**c**) TBUT of healthy group and evaporative DED model mice treated by saline, RosA, Ce^{3+}, RHC, and *s*-RHC group at Day 0, 1, 3, 5, and 7 (n = 5).

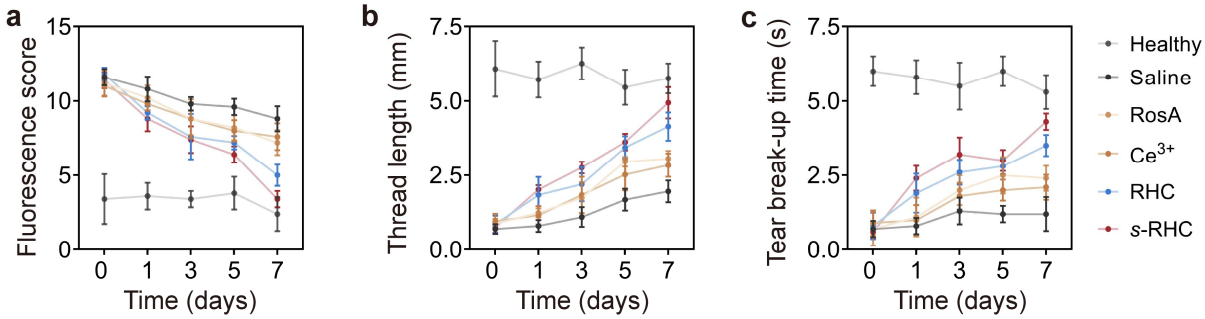

Supplementary Fig. 20. Records of (**a**) fluorescein staining score, (**b**) Schirmer measurement, and (**c**) TBUT of healthy group and aqueous deficient DED model mice treated by saline, RosA, Ce^{3+}, RHC, and *s*-RHC group at Day 0, 1, 3, 5, and 7 (n = 5).

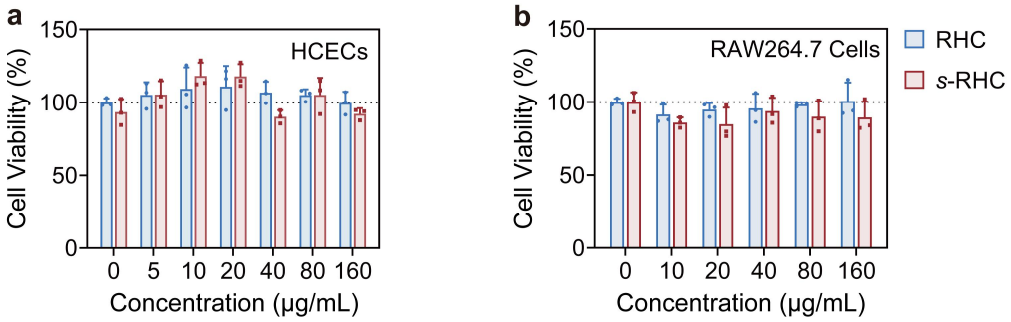

Supplementary Fig. 21. (**a**) Cell viability of HCECs, and (**b**) RAW264.7 cells treated with different concentrations of RHC and *s*-RHC NPs for 24 h (n = 3).

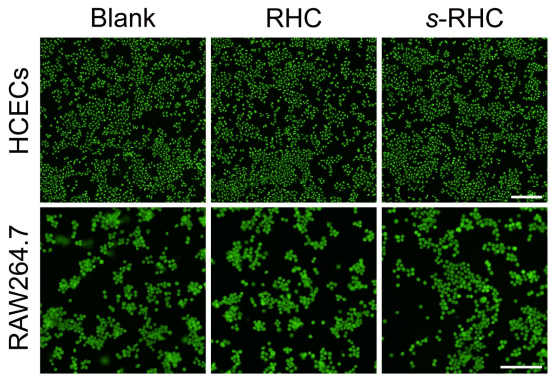

Supplementary Fig. 22. Live/dead cell staining assay of HCECs and RAW264.7 cells treated with different formulations for 24 h. Scale bar (upper) = 500 μm, scale bar (lower) = 100 μm.

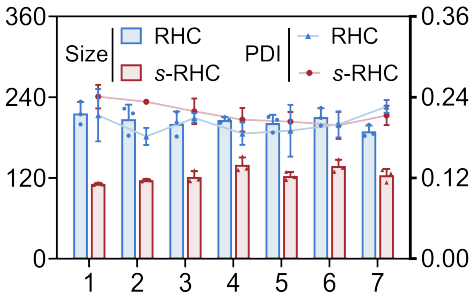

Supplementary Fig. 23. Hydrodynamic size and PDI changes of RHC and *s*-RHC NPs dispersed in water for seven days (stored at 4 °C).

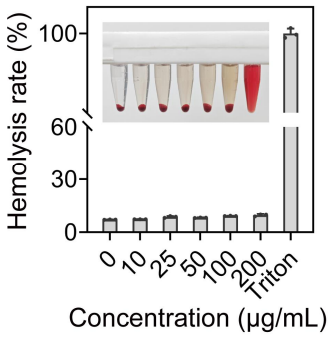

Supplementary Fig. 24. Hemolysis study of *s*-RHC NPs at different concentrations and the digital picture (inset) of precipitated blood cells after incubation.

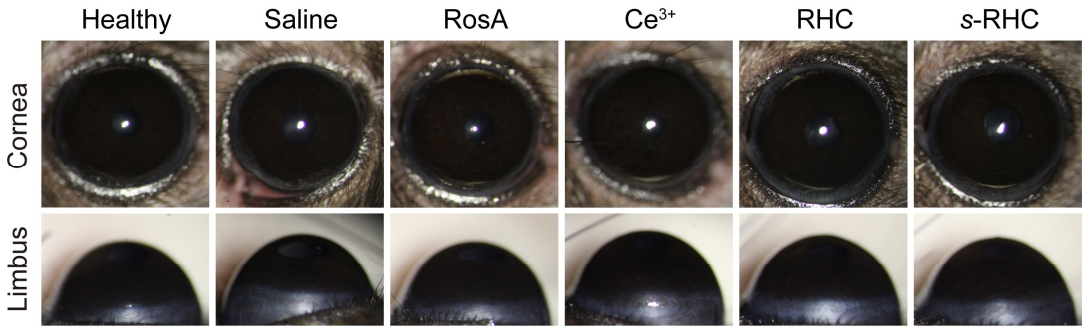

Supplementary Fig. 25. Observation of cornea and limbus of bright light after treating with different formulations at Day 7.

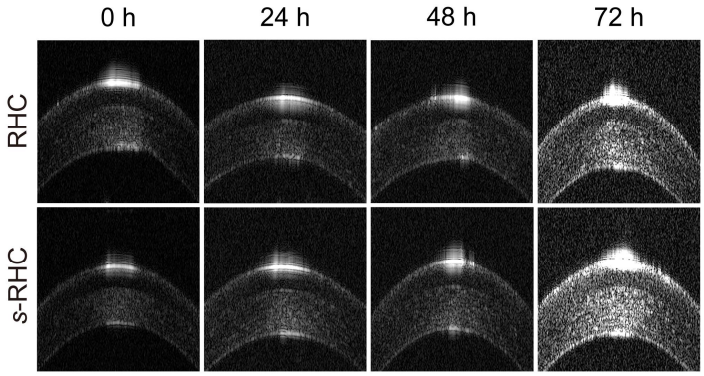

Supplementary Fig. 26. Representative OCT images of the cornea at 0, 24, 48, and 72 h after the topical instillation of RHC and *s*-RHC NPs.

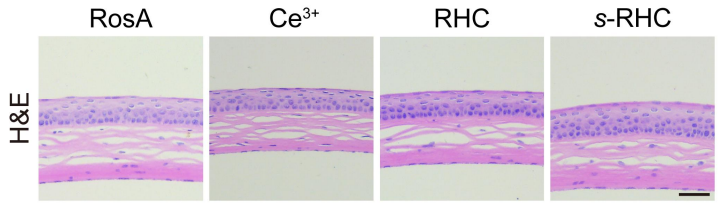

Supplementary Fig. 27. H&E staining results of cornea after administration of RosA, Ce^{3+}, RHC, and *s*-RHC NPs for 72 h. Scale bar = 50 μm.

Supplementary Tables

Supplementary Table 1. Description of symbols of genes and proteins shown in this manuscript.

Symbol	Description
PPP1R15A	Protein Phosphatase 1 Regulatory Subunit 15A
GADD45A	Growth Arrest and DNA Damage Inducible Alpha
JUN	Jun Proto-Oncogene, AP-1 Transcription Factor Subunit
MT-CYB	Mitochondrially Encoded Cytochrome B
MT-ATP6	Mitochondrially Encoded ATP Synthase Membrane Subunit 6
EGR1	Early Growth Response 1
HSPA6	Heat Shock Protein Family A (Hsp70) Member 6
BCL9L	B-Cell Lymphoma 9-Like Protein
BCL2	BCL2 Apoptosis Regulator
BIRC5	Baculoviral IAP Repeat Containing 5
TNFAIP2	TNF Alpha Induced Protein 2
HSPA14	Heat Shock Protein Family A (Hsp70) Member 14
FOSB	FosB Proto-Oncogene, AP-1 Transcription Factor Subunit
HSPA9	Heat Shock Protein Family A (Hsp70) Member 9
SESN2	Sestrin 2
HSPA5	Heat Shock Protein Family A (Hsp70) Member 5
IL17RB	Interleukin 17 Receptor B
IL17B	Interleukin 17B
CASP3	Caspase 3
AP000619.1	Matrix Metallopeptidase 1 (MMP1) Pseudogene
AC024568.1	Heat Shock Protein 90kDa Alpha (cytosolic), Class B Member 1 Pseudogene
FOSL1	FOS Like 1, AP-1 Transcription Factor Subunit
TNFAIP3	TNF Alpha Induced Protein 3
CSF2	Colony Stimulating Factor 2
MMP9	Matrix Metallopeptidase 9
CEBPB	CCAAT Enhancer Binding Protein Beta
MAPK6P3	Mitogen-Activated Protein Kinase 6 Pseudogene 3
CXCL3	C-X-C Motif Chemokine Ligand 3
MMP1	Matrix Metallopeptidase 1
LCN2	Lipocalin 2
MMP3	Matrix Metallopeptidase 3
FOS	Fos Proto-Oncogene, AP-1 Transcription Factor Subunit
PTGS2	Prostaglandin-Endoperoxide Synthase 2
WTAPP1	WTAP Pseudogene 1
CCL17	C-C Motif Chemokine Ligand 17
CXCL18	C-X-C Motif Chemokine Ligand 18

Supplementary Table 2. Ocular irritation test rating scale

Assessment		Score
Corneal opacity	No ulceration or opacity	0
	Scattered or diffuse areas of opacity (other than slight dulling of normal luster); details of iris clearly visible	1
	Easily discernible translucent area; details of iris slightly obscured	2
	Opalescent areas; no details of iris visible, size of pupil barely discernible	3
	Opaque cornea; iris not discernible through the opacity	4
Iritis	Normal	0
	Deepened iris rugae and/or iris congestion or swelling, with	1
	Hemorrhage, gross destruction of iris, or nonreactivity to light	2
Conjunctival redness	Blood vessels normal	0
	Some blood vessels definitely hyperemia (injected)	1
	Diffuse crimson color; individual vessels not easily discernible	2
	Diffuse beefy red	3
Total Score:	Sum of all scores obtained for the cornea, iris, and conjunctivae	